ARL-TR-9769 ● SEP 2023

Investigating Shock Compression Phenomenon Using Laser-Driven Microflyer Plates

by Frank C De Lucia and Debjoy D Mallick

NOTICES

Disclaimers

The findings in this report are not to be construed as an official Department of the Army position unless so designated by other authorized documents.

Citation of manufacturer's or trade names does not constitute an official endorsement or approval of the use thereof.

Destroy this report when it is no longer needed. Do not return it to the originator.

ARL-TR-9769 ● SEP 2023

Investigating Shock Compression Phenomenon Using Laser-Driven Microflyer Plates

Frank C De Lucia and Debjoy D Mallick
DEVCOM Army Research Laboratory

REPORT DOCUMENTATION PAGE

1. REPORT DATE	2. REPORT TYPE	3. DATES COVERED	
		START DATE	END DATE
September 2023	Technical Report	01/01/2023	07/23/2023

4. TITLE AND SUBTITLE
Investigating Shock Compression Phenomenon Using Laser-Driven Microflyer Plates

5a. CONTRACT NUMBER	5b. GRANT NUMBER	5c. PROGRAM ELEMENT NUMBER
5d. PROJECT NUMBER	**5e. TASK NUMBER**	**5f. WORK UNIT NUMBER**

6. AUTHOR(S)
Frank C De Lucia and Debjoy D Mallick

7. PERFORMING ORGANIZATION NAME(S) AND ADDRESS(ES)	8. PERFORMING ORGANIZATION REPORT NUMBER
DEVCOM Army Research Laboratory ATTN: FCDD-RLA-WA Aberdeen Proving Ground, MD 21005	ARL-TR-9769

9. SPONSORING/MONITORING AGENCY NAME(S) AND ADDRESS(ES)	10. SPONSOR/MONITOR'S ACRONYM(S)	11. SPONSOR/MONITOR'S REPORT NUMBER(S)

12. DISTRIBUTION/AVAILABILITY STATEMENT
DISTRIBUTION STATEMENT A. Approved for public release: distribution unlimited

13. SUPPLEMENTARY NOTES
ORCID ID: Frank C De Lucia, 0000-0003-2759-6978

14. ABSTRACT
We are interested in developing a tabletop, high-throughput experiment that will produce well-characterized planar shocks for understanding shock compression in Army-relevant materials. Laser-driven flyer plates can reach velocities on the scale of kilometers/second and deliver reproducible planar microshocks in a laboratory setting on a benchtop. In this study, a high-energy, neodymium-doped yttrium aluminum garnet-pulsed laser (up to 7.5 J, 10-ns pulse) system specifically designed for launching flyer plates is used. The effect of beam shape, beam diameter, and flyer material on the flyer plate launch, flight, and impact is monitored using several diagnostics including photon Doppler velocimetry, high-speed imaging, and light emission collection. It is important to have a well-characterized flyer plate to design experiments for shock compression studies of materials of interest.

15. SUBJECT TERMS
laser-driven flyer plates, photon Doppler velocimetry, energetics, shock compression, Hugoniot, Terminal Effects, Weapons Sciences

16. SECURITY CLASSIFICATION OF:			17. LIMITATION OF ABSTRACT	18. NUMBER OF PAGES
a. REPORT	b. ABSTRACT	C. THIS PAGE		
UNCLASSIFIED	UNCLASSIFIED	UNCLASSIFIED	UU	24

19a. NAME OF RESPONSIBLE PERSON	19b. PHONE NUMBER *(Include area code)*
Frank C De Lucia	(410) 306-0884

STANDARD FORM 298 (REV. 5/2020)
Prescribed by ANSI Std. Z39.18

Contents

List of Figures iv

1. Introduction 1

2. Experimental Approach 2

3. Discussion 6

4. Conclusions 14

5. References 15

List of Symbols, Abbreviations, and Acronyms 17

Distribution List 18

List of Figures

Fig. 1 Experimental layout of laser-driven flyer plate launching and diagnostic optics. Note: APD, avalanche photodiode; bs, beamsplitter; ccd, camera; doe, diffractive optic element; dm, dichroic mirror; el, expansion lens; fl, focusing lens; fpa, flyer plate assembly; m, laser mirror; ml, microscope lens. (Inset) Notional diagram of flyer launch into a target with rear surface velocimetry measurement (left inset) and flyer launch into glass to measure flyer velocity (right inset). 2

Fig. 2 Launching laser beam profile as a function of distance from the focal plane, with positive values denoting a distance from the focal plane that is closer to the focusing lens 4

Fig. 3 High-speed imaging of the flyer launch (side view). High-quality flyer launch as a result of launching from the optimal focus plane (top panels). Low-quality flyer launch as a result of launching 9 mm away from the optimal focus plane (bottom panels). 5

Fig. 4 Side-view, notional diagram of the interaction region within the tamping glass substrate that launches the flyer. The f.l. of the focused launching laser beam affects the potential for breakdown and damage in the substrate when the f.l. is too long and the resulting interaction region is of too little volume. 6

Fig. 5 Spectrogram of PDV signal showing velocity (Y-axis) vs. time (X-axis) of the signal (top). There are two visible tones showing the same velocity history as a result of 1) optical bleed-through, 2) a strong DC harmonic that is interfering with the doppler shifted return signal, or 3) a highly reflecting optic in the velocimetry optics train that is causing unwanted interference. The velocity history can be extracted from the spectrogram as shown here (bottom). 7

Fig. 6 (a) Raw spectrogram of a 0.9-mm-diameter, 25-µm-thick Al plate launch achieving 4.08 km/s launch velocity with subsequent impact into a glass target. (b) Raw spectrogram of a 1.6-mm-diameter, 25-µm-thick Al plate launch achieving 2.4 km/s launch velocity. (c) Raw spectrogram of a 1.2-mm-diameter, 50-µm-thick Al plate launch achieving 2.8 km/s launch velocity. (d) Raw spectrogram of a 1.2-mm-diameter, 25-µm-thick Al plate launch impacting an Al target plate, so only the rear surface/particle velocity history is captured. 9

Fig. 7 Processed particle velocities from PDV 50-µm-thick Cu and Al targets impacted by a 25-µm-thick flyer plate..... 11

Fig. 8 Avalanche detector photodiode emission from flyer plate impacts against glass, RDX, and L-glutamine targets..... 13

1. Introduction

Understanding the phenomena that occur during the extreme conditions resulting from shock compression is important to the US Army Combat Capabilities Development Command (DEVCOM) Army Research Laboratory (ARL). The response of energetic materials to the highly dynamic shock front generated during compression is of particular interest. The interrogation of controlled, reproducible, and well-characterized shock fronts is crucial to studying these responses.[1] Laser-driven flyer plates can be used to produce such shock fronts on a laboratory benchtop with high experimental throughput.[2–7]

In this work, we build on a previous iteration of a benchtop, laser-driven flyer plate system developed at ARL, to achieve higher launch velocities with larger flyer plates.[8] For the new system, we use a high-energy, pulsed neodymium-doped yttrium aluminum garnet (Nd:YAG) laser, in conjunction with specialized optics, to produce a top-hat beam profile optimized for launching laser-driven flyer plates. Our goal is to understand the parameters that affect the maximum velocity that can be obtained to impart the strongest shock compression upon a target material of interest. We examine the effect of beam energy, focus, and profile on velocity and flyer shape. The material, material thickness, and assembly of the launch substrate also have an effect on the flyer plate velocity.[9–11] We use photon Doppler velocimetry (PDV) to accurately measure the velocity of the flyer plate, by using a transparent witness target to monitor the launch, flight, and impact of the flyer.[5,12,13] By using high-speed imaging, we are also able to monitor the flyer plate integrity and morphology in flight and the planarity of the flyer at impact.

We also demonstrate measurements of the particle velocity in the target (the velocity in the target as a result of the imparted shock front) sample after impact using PDV. If the particle velocity is known, we can determine pressure and density in the target sample along the shock front with either the Hugoniot data of the material or the shock velocity (U_S).[3,14–19]

The emissions from the impact are also of interest, especially for energetic materials.[8] The ability to capture the emissions using an avalanche photodiode allows us to observe emission differences from material to material. Coupling these various diagnostics into the new laser-driven flyer experimental system allows us to develop a complete picture and understanding of the parameters that affect the flyer plate launch, flight, and impact, in turn enabling the design of experiments for investigating shock compression in a variety of materials of interest to the Army.

2. Experimental Approach

The laser-driven flyer plate experimental layout is shown in Fig. 1. It is divided into three different sections: 1) the launch optics, 2) flyer plate assembly, and 3) the diagnostics. An Nd:YAG-pulsed laser system (Titan 6, Amplitude Technologies) produces a quasi-top-hat, 1064-nm, 10-ns laser pulse with a maximum energy of 7.5 J and a beam diameter of 20.5 mm. A single shot from the laser is used to launch the laser-driven flyer plate. The laser pulse passes through beam expansion optics that increase the beam diameter to 54.5 mm. Then, the pulse passes through a focusing lens into a diffractive optic element (DOE). The DOE is an off-axis, 70.5-mm-diameter homogenization element with a 12.5-mrad divergence that produces a round, top-hat beam profile at the focal point. The diameter of the top-hat beam at the focus is defined by the following:

$$\Theta * \text{f.l.} = \text{beam diameter},$$

where Θ is the divergence in mrad, f.l. is the focal length of the lens in meters, and the beam diameter is in millimeters.

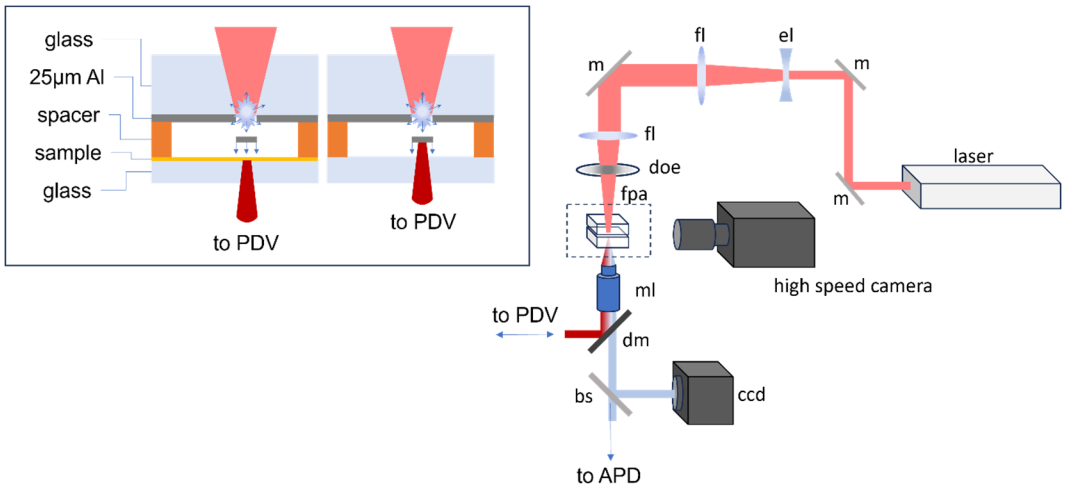

Fig. 1 Experimental layout of laser-driven flyer plate launching and diagnostic optics. Note: APD, avalanche photodiode; bs, beamsplitter; ccd, camera; doe, diffractive optic element; dm, dichroic mirror; el, expansion lens; fl, focusing lens; fpa, flyer plate assembly; m, laser mirror; ml, microscope lens. (Inset) Notional diagram of flyer launch into a target with rear surface velocimetry measurement (left inset) and flyer launch into glass to measure flyer velocity (right inset).

The flyer plate assembly is made up of two main parts: 1) the material that will be used as the flyer plate affixed to a substrate and 2) the target material on a different substrate separated by a spacer. The flyer plate assemblies are assembled using a 3/4-inch borosilicate glass block as the substrate. An optically clear adhesive (Loctite 4601) is used to affix the aluminum flyer material (typically 25 μm thick) to the glass. We spread a thin layer of the adhesive—just a couple of drops spread around the glass evenly—and then press the glass block onto the aluminum, squeezing the assembly between two plastic blocks that are held together by clamps until the adhesive has reached full strength. We wait at least 24 h before using the flyer plate launch assembly so that the adhesive is adequately cured. To perform a successful launch, the launching laser pulse is focused onto the glass–adhesive–aluminum interface, forming a rapidly expanding mixture of plasma and ablated material as shown in the inset of Fig. 1. Eventually, as the pressure of the expanding mixture overcomes the tensile strength of the glass–adhesive–aluminum interface, it punches out an aluminum disk at an extremely high velocity (hundreds of m/s). The distance between launch and the target is determined by a spacer (<1 mm) that is sandwiched between the launched aluminum surface and the target material. There are numerous configurations that can be used for the target material, but typically it is a thin (<100 μm) sample, so a sustained planar shock can traverse the entire sample.

For velocimetry, our PDV diagnostic can be described as a fiber-coupled Michelson interferometer, where the flyer plate acts as the moving mirror. (A more detailed description of PDV can be found in Dolan.[12]) We use a modified PDV system described by Mallick et al.[13,20] that images the PDV laser (NKT Basik 1550.12 nm operating at 45 mW output) through a microscope objective (COMPUTAR SWIR f = 25 mm) and onto the flyer plate and collects the reflected PDV laser during the experiment. The primary departure of our system from a conventional PDV system is in a high-gain amplifier (Lumibird) used to amplify the returned signal prior to the interference step. In addition to collecting velocimetry, the microscope objective also interrogates emission from the impact of the flyer with the target. The emission is separated from the PDV laser by a dichroic mirror; it passes through a 50:50 beamsplitter and then focuses onto a fiber. The light travels through a fiber and is attenuated by an in-line fiber optic filter mount before reaching an Si variable-gain APD detector (Thorlabs, APD410A).

A camera is also cowitnessed through the microscope objective to enable careful alignment of the flyer plate assembly, the target, and the in situ diagnostics. Separate from the diagnostics that are cowitnessed through the microscope objective, a high-speed framing camera (Shimadzu HPV-X2) is used to capture the launch, flight, and impact of the flyer plate from the side view. The framing camera uses a 100-mm camera objective coupled to a teleops doubler. The framing camera image is illuminated from behind the experiment region using an illumination laser (Cavitar Cavilux Smart UHS, 810 nm).

We use a laser beam profiler (Newport, LBP2-VIS2) to analyze the beam shape after the DOE. A 150-mm lens focuses the beam through the DOE onto the beam profiler. We collect beam profiles at different distances relative to the focal point of the focusing lens/DOE combination to find the "best" top-hat profile, as shown in Fig. 2. The beam profile denoted as 0 mm is the profile with the optimal top-hat shape at the focal point of the combined focusing lens and DOE. The beam shape changes as the beam profiler moves further away from the focal plane. With this series of beam profiles, we know where to place our flyer plate assembly relative to the DOE to achieve the optimal top-hat beam shape at the glass–aluminum interface. We also observe that the top-hat shape is still maintained at ±1 mm so there is some leeway in where the flyer plate launch layer is placed relative to the DOE. Using the laser beam profiler, we determine that the diameter of the top-hat profile is approximately 1.5 mm.

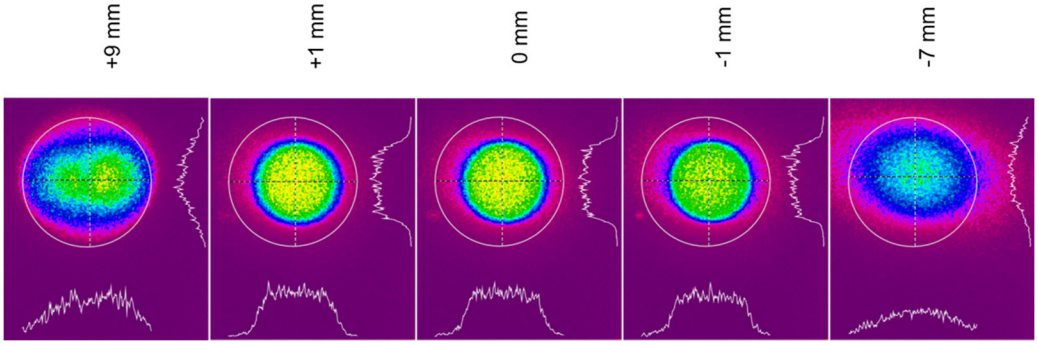

Fig. 2 Launching laser beam profile as a function of distance from the focal plane, with positive values denoting a distance from the focal plane that is closer to the focusing lens

In the top panels of Fig. 3, we show images from a high-speed video of a 25-µm-thick Al flyer that is launched by a top-hat, 4.7-J laser pulse. The first image of the flyer is after the aluminum has detached from the launch substrate. The second image of the flyer is collected at impact with the glass substrate target. In the bottom panels of Fig. 3, we show images of a flyer that is launched using the beam profile in Fig. 2 that is +9 mm above the optimal focus towards the DOE. The first image shows how the shape of the flyer is influenced by the beam profile shape. In this case, instead of a flat flyer plate, we end up with a larger flyer that has two distinct rounded bumps. Thus, the flyer cannot deliver a planar shock wave across the target upon impact.

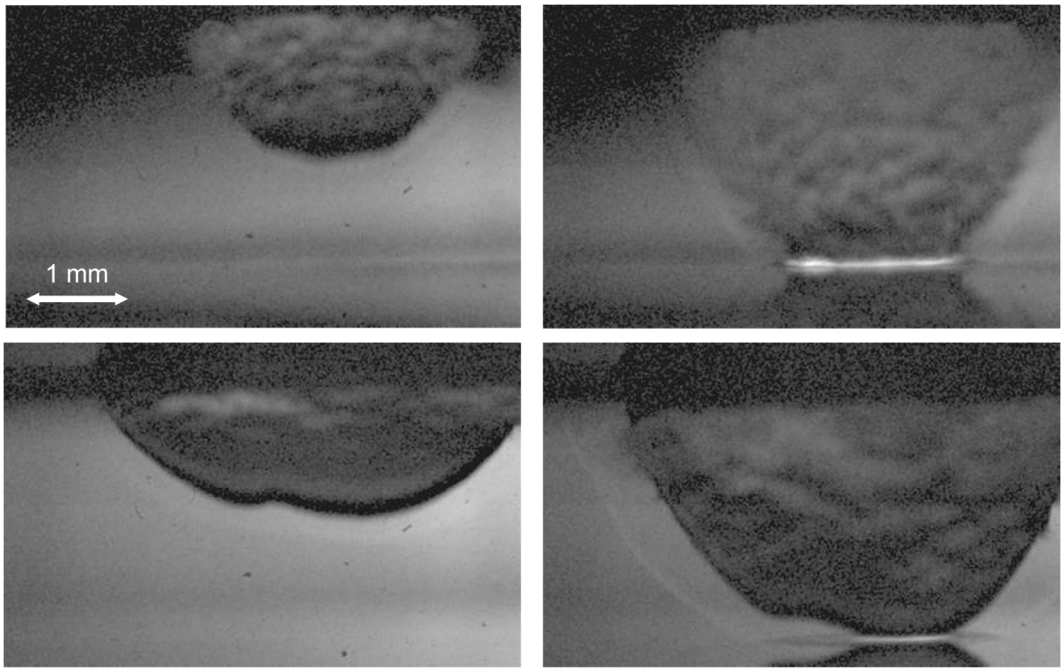

Fig. 3 High-speed imaging of the flyer launch (side view). High-quality flyer launch as a result of launching from the optimal focus plane (top panels). Low-quality flyer launch as a result of launching 9 mm away from the optimal focus plane (bottom panels).

We use the 3/4-inch glass as the backing substrate to the launched aluminum flyer to minimize breakdown on the air–glass interface on the opposite side of the glass–aluminum interface. As the laser beam is focused onto the target, the energy density increases, as illustrated in Fig. 4. As the substrate thickness increases, the beam area at the air–glass interface slightly increases; therefore, the energy density is smaller. This is why we observe more breakdown on the air–glass interface of thin glass substrates used in flyer plate launch assemblies. Less energy is able to reach the glass–aluminum interface, and thus the maximum plate velocity decreases. We want to increase the beam diameter at the air–glass interface to limit plasma formation, so we expand the beam diameter, using a combination of focusing and expanding lenses, from 20.5 to 54.5 mm. In the right image of Fig. 4, the beam area at the air–glass surface has increased due to the expanded beam.

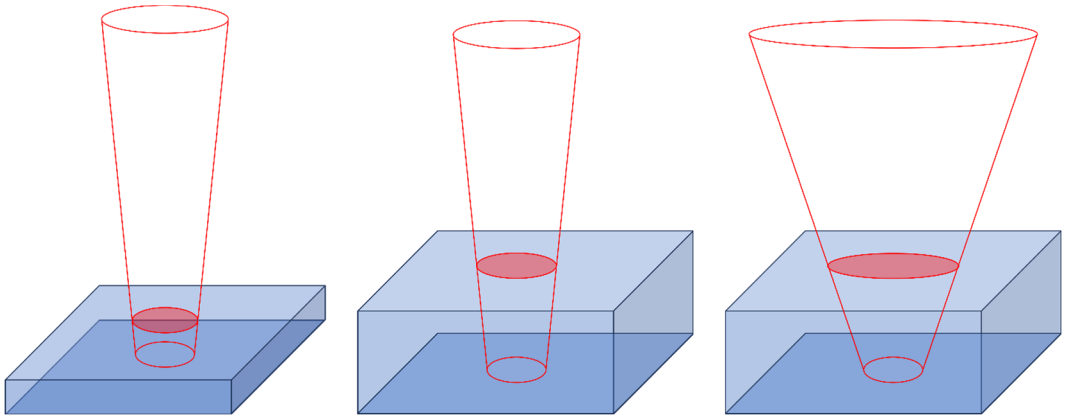

Fig. 4 Side-view, notional diagram of the interaction region within the tamping glass substrate that launches the flyer. The f.l. of the focused launching laser beam affects the potential for breakdown and damage in the substrate when the f.l. is too long and the resulting interaction region is of too little volume.

3. Discussion

To characterize the flyer plate launch, we used borosilicate glass as the target so the PDV laser can view the flyer plate in motion through the transparent glass. The configuration is shown in the inset in Fig. 1, top right. We used SIRHEN 2, a data reduction program that essentially uses various Fourier transform techniques to process the returned voltage signal, for extracting velocity profiles from PDV measurements.[21] In Fig. 5, we show the raw spectrogram and the processed velocity trace extracted from a PDV measurement from an Al flyer plate impacting glass. The flyer is a 1-mm-diameter, 25-µm-thick Al and is launched by a 4.9-J top-hat laser pulse. The gap between the flyer launch assembly and the target glass is 500 µm. During the beginning of the launch, the flyer is punched away from the foil and rapidly accelerates for the first 40 ns. Then, the velocity continues to

increase to the maximum velocity of approximately 4 km/s before it impacts with the glass target, indicated by a sudden drop in velocity. From this velocity trace we can also obtain the particle velocity (U_p)—one of the parameters used to describe the Hugoniot of a material.[18]

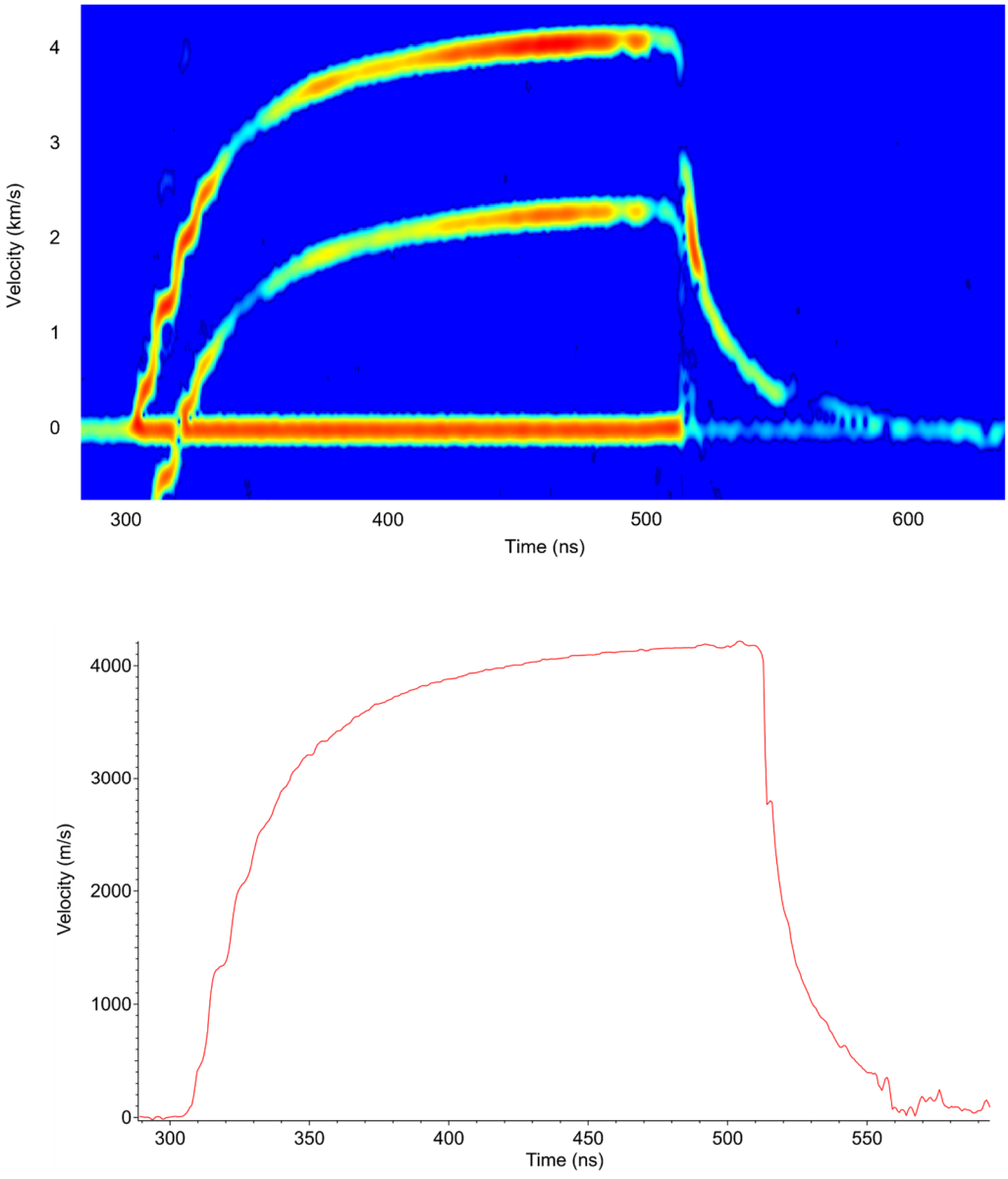

Fig. 5 Spectrogram of PDV signal showing velocity (Y-axis) vs. time (X-axis) of the signal (top). There are two visible tones showing the same velocity history as a result of 1) optical bleed-through, 2) a strong DC harmonic that is interfering with the doppler shifted return signal, or 3) a highly reflecting optic in the velocimetry optics train that is causing unwanted interference. The velocity history can be extracted from the spectrogram as shown here (bottom).

U_p is determined from the velocity observed immediately after impact, because this is when the flyer is pushing the target material (in this case the glass). The particle velocity is reduced relative to the flyer plate velocity. The amount the velocity is reduced is based on the impedance of the flyer plate and the target material.[19] The observed velocity, estimated to be 2.8 km/s, is the small shoulder marked by an arrow in Fig. 5. A thicker flyer plate would lead to a longer shock duration and thus a longer-lived "shoulder" to measure U_p. The "shoulder" for this 25-µm-Al plate impact is approximately 1.9 ns; using a 50-µm-Al plate leads to a "shoulder" of 4.4 ns (not pictured).

In Fig. 6, we show the raw PDV trace from several different flyer plate launches and configurations. Figure 6a is the PDV trace collected from a 0.9-mm-diameter, 25-µm-thick Al flyer plate that reaches a maximum velocity of 4.08 km/s. The flyer traverses a 500-µm gap between the launch substrate surface and the target glass surface. In Fig. 6b, we observe the PDV trace from a 1.6-mm-diameter, 25-µm-thick Al flyer plate that reaches a maximum velocity of 2.4 km/s. However, in this case, we do not see the impact because the gap is 2.3 mm. At 2.4 km/s, it takes approximately 950 ns to travel across that gap, and our PDV window is only 800 ns. The PDV trace in Fig. 6c is a 1.2-mm-diameter, 50-µm-thick Al flyer plate that reaches a maximum velocity of 2.8 km/s. It is crossing a gap of 760 µm before impact with the glass target. Finally, in Fig. 6d, we observe the PDV trace from the back of an aluminum target, impacted by a 1.2-mm-diameter, 25-µm-thick Al flyer plate. Because the target in this case is a 25-µm-thick Al foil, the PDV cannot observe the flyer plate flight. We only observe the breakout shock due to the impact of the flyer with the target foil. This velocity, 2.1 km/s, is the U_p described previously.

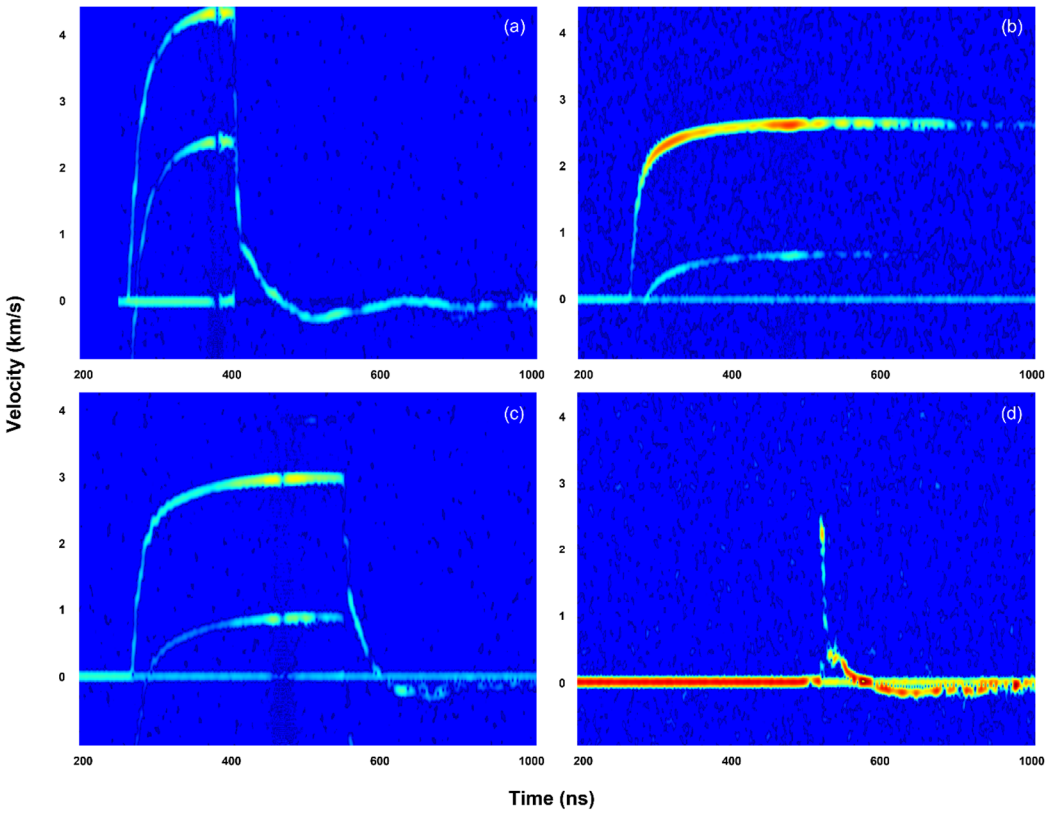

Fig. 6 (a) Raw spectrogram of a 0.9-mm-diameter, 25-µm-thick Al plate launch achieving 4.08 km/s launch velocity with subsequent impact into a glass target. (b) Raw spectrogram of a 1.6-mm-diameter, 25-µm-thick Al plate launch achieving 2.4 km/s launch velocity. (c) Raw spectrogram of a 1.2-mm-diameter, 50-µm-thick Al plate launch achieving 2.8 km/s launch velocity. (d) Raw spectrogram of a 1.2-mm-diameter, 25-µm-thick Al plate launch impacting an Al target plate, so only the rear surface/particle velocity history is captured.

The flyer plate assemblies described in Section 2 are a simple design. An adhesive is used to hold a thin foil to the glass substrate, typically a 2- × 2-inch borosilicate glass block that is 3/4 inches thick. We find that for a given flyer plate assembly, the flyer plate velocity is repeatable. However, the velocity from assembly to assembly can be quite different. For example, we use an epoxy (Loctite Ablestik 24) to make three different flyer plate assemblies: A, B, and C. Because the epoxy application is not controlled in any quantifiable method apart from the number of drops of epoxy, each assembly has a different amount of adhesive and curing pressure.

The flyer plate velocities launched from assemblies A, B, and C are 3.25 ± 0.06 (95% confidence limit), 2.83 ± 0.13, and 1.86 ± 0.05 km/s, respectively. Furthermore, we use a simple optically clear super glue to build several additional assemblies. For one assembly, we apply one drop per square inch (4 drops total) and then pressed the glass block onto the Al foil (Assembly no. 1).

For another assembly, we apply two drops and then spread the glue thinly to cover the whole glass surface before pressing it to the Al foil (Assembly no. 2). The plate velocities obtained from Assembly nos. 1 and 2 were 3.73 ± 0.06 (95% confidence limit) and 3.99 ± 0.08 km/s, respectively. The optimal flyer plate assembly method is achieved by using the minimum amount of adhesive that also evenly covers the 2- × 2-inch glass surface. It is imperative to measure the flyer velocity from a newly made flyer plate assembly before beginning experiments.

When a nontransparent sample is the target, the PDV cannot measure the flyer plate velocity. Thus, it is important to establish the flyer plate velocity from the flyer plate assembly that will be used in the experiment with a transparent target. In Fig. 7, we show the PDV traces captured from the impact of a 25-μm flyer plate with 50-μm-thick copper and aluminum. We first find the velocity of the flyer plates, 3.07 ± 0.05 km/s, using just glass as the target. Next, the PDV is focused onto the bottom of the target sample. The PDV measures the U_p of the metal foil (Cu or Al) at the metal–glass interface as shown in Fig. 1 inset. This is where the shock breaks out of the metal into the glass substrate.

The peak velocity in Fig. 7 of the aluminum and copper is the U_p of the materials due to the flyer plate impact and subsequent shock that is transferred into the thin metal foil, 1.95 and 1.52 km/s respectively. The lower particle velocity for copper is because the particle velocity is related to the shock impedance of the aluminum flyer plate and the target material. With the U_p value and Hugoniot data[18] of each material, the Rankine–Hugoniot equations can be used to estimate the pressure and density behind the shock front (with some assumptions).[3,18,22]

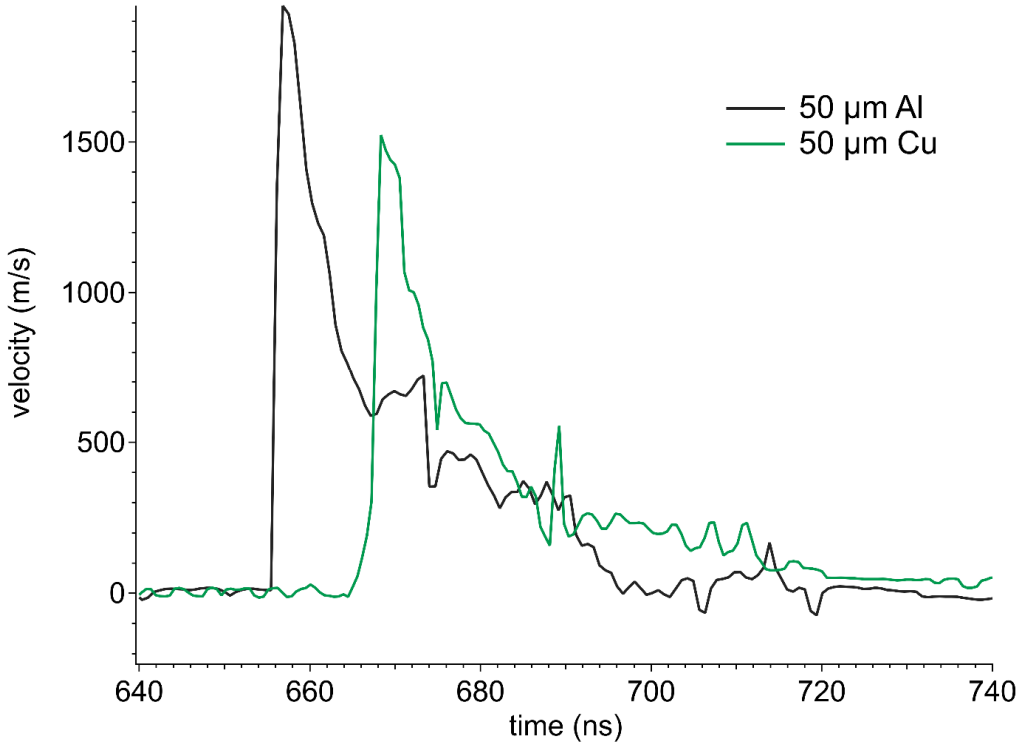

Fig. 7 Processed particle velocities from PDV 50-µm-thick Cu and Al targets impacted by a 25-µm-thick flyer plate

Although U_p is relatively straight forward to determine from laser-driven flyer plate experiments, if Hugoniot data is not available, to solve Rankine–Hugoniot equations, another factor is needed. Typically, U_s is used because it can be measured simultaneously with U_p in a single flyer plate experiment. It is difficult to obtain U_s because it requires a known distance and precise time measurement. In larger experiments, this is more straightforward because pressure gauges can be used at fixed distances.

For laser-driven flyer plate experiments, a thin and transparent sample is necessary, so the PDV can see the impact at the surface of the sample and then the breakout shock at the other side of the sample.[16,17] This limits the possible samples that might be studied with this approach. In future studies, we will investigate different sample configurations to try to obtain accurate U_s values from nontransparent samples with laser-driven flyer plates.

In Fig. 8, top panel, we show the APD trace collected from a flyer plate launch and impact with glass as a target. The first peak is due to the initial laser flash and light from the laser plasma. The second peak originates from the flyer impact on the glass. We launch 25-μm-thick, 1.2-mm-diameter flyer plates with a velocity of 3.05 km/s at glass, 1,3,5-trinitro-1,3,5-triazinane (RDX), and L-glutamine. The RDX and L-glutamine are loosely packed into 50-μm-deep, 1.5-mm-diameter cylindrical wells cut from Kapton tape that is affixed to the glass substrate.

We do not attempt to quantify the RDX or L-glutamine. The APD traces of the glass, RDX, and L-glutamine are shown in Fig. 8, bottom panel. We observe that the first peak due to the initial laser flash is present in all three samples. The second peak is observed in the glass and RDX samples, but this is not present in the L-glutamine, indicating that the powder perhaps obscures or diminishes the light due to impact compared to the other two samples. RDX has more emission after the sample, which could be indicative of burning particles or other combustion products that we would not see with L-glutamine because it is an inert organic material. Additional experiments will be performed to investigate the differences in emission of energetic materials compared to nonenergetic materials due to flyer impact.

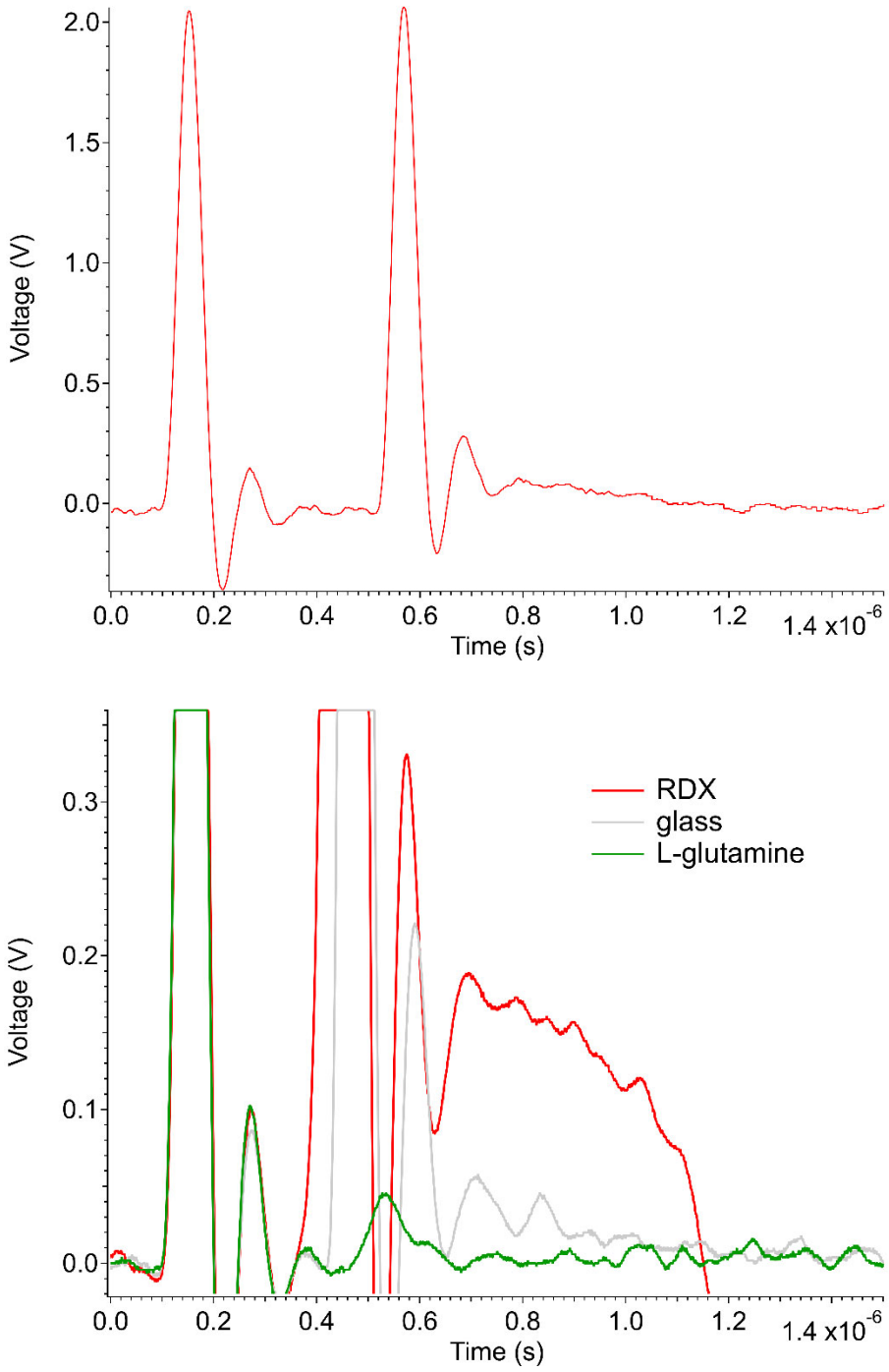

Fig. 8 Avalanche detector photodiode emission from flyer plate impacts against glass, RDX, and L-glutamine targets

4. Conclusions

In this work, we described the laser-driven flyer plate system developed at ARL, including control of beam diameter and profile, flyer plate launch assembly, and diagnostics. PDV is used to measure the flyer plate velocities and the breakout particle velocities measured after flyer impact. We have shown how the adhesive coverage from one flyer plate assembly to another alters the flyer plate velocity. Although the flyer plate velocities within an individual flyer plate assembly are relatively similar, the flyer plate diameter and backing substrate thickness also influence the flyer plate velocity. The particle velocity is measured after the flyer impact and appears as a shoulder in the PDV trace of an impact with a transparent target. When the target is not transparent, only the breakout velocity is observed in the PDV trace. Here, the particle velocity is represented by the peak of the velocity trace, as observed in Fig. 6d and Fig. 7. Finally, we capture the emission of the impact with several samples using an APD. We observe increased emission due to RDX, possibly due to burning particles not observed in the other samples.

Further studies will involve developing a method to measure the shock velocities with high accuracy. Even small differences in the measurements can alter the calculated U_s measurements. In addition, we will focus on determining the particle velocities for energetic materials (and inert organic materials for comparison) using a range of flyer plate velocities. In particular, we are interested in any relationship between particle velocity and energetic characteristics. During these studies, we will also monitor the emission profile of the energetics (and nonenergetics) to observe how emission changes over a range of flyer plate velocities.

5. References

1. Trott WM, Erickson KL. Ultra-high-speed studies of shock phenomena in a miniaturized system: a preliminary evaluation. Sandia National Laboratories (US); 1997. Report No.: SAND97-2214 .
2. Paisley DL. Laser-driven miniature flyer plates for shock initiation of secondary explosives. Los Alamos National Laboratory (US); 1989. Report No.: LA-UR-89-2723 .
3. Swift DC, Niemczura JG, Paisley DL, Johnson RP, Luo S, Tierney TE. Laser-launched flyer plates for shock physics experiments. Rev Sci Instrum. 2005;76 (9):093907.
4. Paisley DL, Luo SN, Greenfield SR, Koskelo AC. Laser-launched flyer plate and confined laser ablation for shock wave loading: validation and applications. Rev Sci Instrum. 2008;79(2):023902.
5. Curtis AD, Banishev AA, Shaw WL, Dlott DD. Laser-driven flyer plates for shock compression science: launch and target impact probed by photon Doppler velocimetry. Rev Sci Instrum. 2014;85(4):12.
6. Dlott DD. Laser pulses into bullets: tabletop shock experiments. Phys Chem Chem Phys. 2022;24(18):10653–10666.
7. Li F, Dlott DD. High throughput tabletop shock techniques and measurements. J Appl Phys. 2022;131(7):075901.
8. Dean SW, De Lucia FC Jr, Gottfried JL. Indirect ignition of energetic materials with laser-driven flyer plates. Appl Opt. 2017;56(3):B134–B141.
9. Watson S, Field JE. Integrity of thin, laser-driven flyer plates. J Appl Phys. 2000;88(7):3859–3864.
10. Sheffield SA, Rogers JW, Castañeda JN. Velocity measurements of laser-driven flyers backed by high impedance windows. Shock waves in condensed matter. Gupta YM, editor. Springer US; 1986. p. 541–546.
11. Stahl DB, Gehr RJ, Harper RW, Rupp TD, Sheffield SA, Robbins DL. Flyer velocity characteristics of the laser-driven miniflyer system. 1999 APS Topical Conference on Shock Compression of Condensed Materials; 1999 June 27–July 2; Snowbird, Utah.
12. Dolan DH. Extreme measurements with photonic doppler velocimetry (PDV). Rev Sci Instrum. 2020;91(5):051501.

13. Mallick DD, Zhao M, Bosworth BT, Schuster BE, Foster MA, Ramesh KT. A simple dual-beam time-multiplexed photon doppler velocimeter for pressure-shear plate impact experiments. Expt Mech. 2019;59(1):41–49.

14. Warnes RH, Paisley DL, Tonks DL. Hugoniot and spall data from the laser-driven miniflyer. Proceedings of the Conference of the American Physical Society Topical Group on Shock Compression of Condensed Matter; 1995 Aug 13–18; Seattle, WA. p. 495–498.

15. Trott WM, Setchell RE, Farnsworth JAV. Development of laser-driven flyer techniques for equation-of-state studies of microscale materials. AIP Conference Proceedings. 2002;620(1):1347–1350.

16. Brown KE, Shaw WL, Zheng X, Dlott DD. Simplified laser-driven flyer plates for shock compression science. Rev Sci Instrum. 2012;83(10):103901–103913.

17. Fujiwara H, Brown K, Dlott D. A thin-film Hugoniot measurement using a laser-driven flyer plate. AIP Conference Proceedings. 2012;1426:382–385.

18. Marsh SP. LASL shock Hugoniot data. University of California Press, Berkeley; 1980.

19. Ito K, Aizawa T, Paisley DL. Laser-driven shock device for real-time Hugoniot measurement. Koatsuryoku no Kagaku to Gijutsu. 1998;7:876–878.

20. Mallick DD, Zhao M, Parker J, Kannan V, Bosworth BT, Sagapuram D, Foster MA, Ramesh KT. Laser-driven flyers and nanosecond-resolved velocimetry for spall studies in thin metal foils. Expt Mech. 2019;59(5):611–628.

21. Dolan I, Daniel H, Ao T. SIRHEN: a data reduction program for photonic Doppler velocimetry measurements. Sandia National Laboratories (US); 2010. Report No.: SAND2010-3628.

22. Sellan D, Zhou X, Salvati L, Valluri SK, Dlott DD. In operando measurements of high explosives. J Chem Phys. 2022;157(22):224202.

List of Symbols, Abbreviations, and Acronyms

APD	avalanche photodiode
ARL	Army Research Laboratory
DEVCOM	US Army Combat Capabilities Development Command
DOE	diffractive optical element
f.l.	focal length
mrad	milliradian
Nd:YAG	neodymium-doped yttrium aluminum garnet
PDV	photon Doppler velocimetry
RDX	1,3,5-trinitro-1,3,5-triazinane
U_p	particle velocity
U_s	shock velocity

1 (PDF)	DEFENSE TECHNICAL INFORMATION CTR DTIC OCA
1 (PDF)	DEVCOM ARL FCDD RLB CI TECH LIB
6 (PDF)	DEVCOM ARL FCDD RLA W T SHEPPARD FCDD RLA WA F DELUCIA N DANG J GOTTFRIED S DEAN FCDD RLA TF D MALLICK